Rheological characterization of compatibilized polymer blends

Aurélie Taguet

▶ **To cite this version:**

Aurélie Taguet. Rheological characterization of compatibilized polymer blends. Compatibilization of Polymer Blends, Elsevier, pp.453-487, 2019, 978-0-12-816006-0. 10.1016/B978-0-12-816006-0.00016-5 . hal-02514987

HAL Id: hal-02514987

https://imt-mines-ales.hal.science/hal-02514987

Submitted on 5 Jun 2023

HAL is a multi-disciplinary open access archive for the deposit and dissemination of scientific research documents, whether they are published or not. The documents may come from teaching and research institutions in France or abroad, or from public or private research centers.

L'archive ouverte pluridisciplinaire **HAL**, est destinée au dépôt et à la diffusion de documents scientifiques de niveau recherche, publiés ou non, émanant des établissements d'enseignement et de recherche français ou étrangers, des laboratoires publics ou privés.

Rheological characterization of compatibilized polymer blends

Aurélie Taguet
C2MA, IMT Mines Ales, University of Montpellier, Ales, France

Abbreviations

CB	Carbon black
CMC	Critical micelle concentration
CNT	Carbon nanotube
DM	Dodecyl mercaptan
EPDM	Ethylene propylene diene monomer
EPM-*g*-MA	Maleic anhydride–grafted ethylene propylene monomer
ER	Epoxy resin
EVA	Poly(ethylene-*co*-vinyl acetate)
EVOH	Poly(ethylene-*co*-vinyl alcohol)
GS	Grafted silica
HDPE	High-density polyethylene
HDPE-*g*-MA	High-density polyethylene-grafted maleic anhydride copolymer
HIPS	High-impact polystyrene
JGS	Janus-grafted silica nanoparticle
JPs	Janus particles
LDPE	Low-density polyethylene
LIR	Liquid isoprene rubber
MA	Maleic anhydride
MAPP	Maleic anhydride–grafted polypropylene
MHDPE	Modified HDPE
mLLDPE	Metallocene-catalyzed linear low-density PE
MPS	γ-methacryloxypropyltrimethoxysilane
MWCNT	Multiwall carbon nanotube
NP, NPs	Nanoparticle, nanoparticles
NPFP	Nanoparticle-filled polymer
OTS	Octadecyltrichlorosilane
P((S-*co*-GMA)-*g*-MMA)	Poly(styrene-*co*-glycidyl methacrylate)-graft-poly(methyl methacrylate)
PA	Polyamide
PA 12	Polyamide 12
PA 6	Polyamide 6
PA 66	Polyamide 6,6
PB	Polybutadiene
PBAT	Poly(butylene adipate-*co*-terephthalate)

PBS	Poly(butylene succinate)
PBSA	Poly(butylene succinate-*co*-adipate)
PBT	Polybutylene terephthalate
PC	Polycarbonate
PCL	Poly(ε-caprolactone)
PDMS	Polydimethyl siloxane
PDVB	Polydivinylbenzene
PE	Polyethylene
PEO	Polyethylene oxide
PET	Poly(ethylene terephthalate)
PETG	polyethylene terephthalate glycol
PI	Polyisoprene
PIB	Polyisobutylene
PLA	Poly(lactic acid)
PLA-*g*-MA	Polylactic acid—grafted maleic anhydride
PLLA	Poly(L-lactic acid)
PLLA-*b*-PGMA	PLLA-block-poly(glycidyl methacrylate)
PMMA	Poly(methyl methacrylate)
POE	Ethylene—octene copolymer
POSS	Polyhedral oligomeric silsesquioxane
PP	Polypropylene
PPE	Poly(2,6-dimethyl-1,4-phenylene ether)
PS	Polystyrene
PSAN	Poly(styrene-*co*-acrylonitrile)
PTT	Polytrimethylene terephthalate
PVDF	Polyvinylidene fluoride
SAN	Styrene—acrylonitrile
SBM	Triblock terpolymer polystyrene-block-polybutadiene-block-poly (methyl methacrylate)
SBR	Styrene—butadiene rubber
SEBS	Styrene—ethylene—butylene—styrene block copolymer
SEBS-*g*-MA	Styrene—ethylene—butylene—styrene block copolymer—grafted maleic anhydride
SEM	Scanning electron microscope
SMA	Poly(styrene-*co*-maleic anhydride)
TEM	Transmission electron microscope
TPE	Thermoplastic elastomer

16.1 Introduction

Rheology is the science of deformation and flow of matter, especially liquids and soft matter. Concerning polymers it is the science of their flow in the melting state for thermoplastics and prior to cross-linking for the thermosets and elastomers. The rheological behavior of polymers is specifically studied in order to investigate the structure and spacial arrangement

of the macromolecules that tells us about the different intra- and intermolecular interactions [1]. Moreover, rheological measurements are performed on polymers in order to assess for their behavior during processing [2]. Rheological characterization can be used to fix the optimum process. In polymer blends and alloys, due to the influence of a high number of parameters (such as concentration, morphology, flow geometry, interactions of each phase), the rheological behavior is complex and sometimes difficult to relate to the intrinsic physical properties of the fluid [3]. The addition of a compatibilizer, in order in fine, to get higher macroscopic mechanical, thermal, electrical, fire properties, dramatically influences the rheology of the blend. This compatibilizer can be a copolymer (either inert such as block copolymers or reactive) or a filler. The rheological behavior of those three different routes of compatibilization will be described in the present chapter. And the examples and conclusions are most of the time limited to thermoplastics in the molten state or elastomers in the liquid state.

Three types of flow are mainly used in the rheological measurements of polymer blends: steady state shearing, dynamic shearing, and elongation. These models are varied regarding their shear rate and the uniformity of the stress and strain. In the present chapter, only steady state and dynamic shears will be studied. Most of the polymer blends cited in the present chapter are immiscible or partially miscible.

In the first part, general outlines concerning the rheology of polymer blends are rapidly drawn. Then, the case of compatibilization by copolymers is detailed in the second part, differentiating the rheological influence of block copolymers (16.3.1) to that of reactive copolymers (16.3.2). The special case of rheology of cocontinuous compatibilized blends is exposed in 16.3.3. In the third part (16.4), the compatibilization by fillers, and particularly nanofillers, is largely exposed. A short paragraph recalls rapidly the generalities concerning the rheological behavior of polymer-based nanocomposites (16.4.1). Then, the importance of the localization of the fillers in the polymer blends has been emphasized (16.4.2). The case of spherical silica nanoparticles (NPs) is developed (16.4.2) followed by plate- and tube-shape NPs (16.4.4). Finally, Janus particles as compatibilizers are exposed in 16.4.5.

16.2 Generalities on rheology of polymer blends

Heterogeneous polymer blends in the molten state are considered as emulsions, especially the shape of the dispersed phase can change during

deformation and this can be well-characterized by rheological tests. In the case of droplets (dispersed phase) into a continuous matrix, the balance of the viscous forces outside the particles and the Laplace pressure originating from the interfacial tension determine the equilibrium form of the inclusions. The capillary number *Ca* and the viscosity ratio *p* can be calculated to determine the capacity of deformation of the drop.

$C_a = \eta_m \dot{\gamma} R / \Gamma$ and $p = \frac{\eta_d}{\eta_m}$, where η_m and η_d are the viscosities of the matrix and dispersed phase, respectively. $\dot{\gamma}$ is the strain rate, R the drop radius, and Γ the interfacial tension.

These two parameters are crucial to determine the final morphology of the blend. For example, dispersion is finer if the minor component has a lower viscosity compared to the major one [4]. The interactions between separate phases may affect the viscous and elastic behavior and hence the rheological behavior of the blend. Moreover, the elastic properties of the system were found to be more sensitive to the state of dispersion than the viscous properties of the blends [5].

The deformability of the dispersed phases and their coalescence can lead to a wide variety of morphology changing that affects rheological properties especially at low frequency or low shear rate. Indeed, it is often observed that the blend loses its Newtonian behavior at low frequency (or shear rate) and the effect of flow-induced molecular orientation on the viscosity and elasticity becomes more important. Hence, the influences of the dispersed phases on the viscosity decreases with increasing shear rates [3]. For immiscible polymer blends, there are several common mixing rules to predict the viscosity of the blend regarding the viscosity of each component: additivity model, log additivity model, and fluidity model [6]. It is commonly recognized that the additivity model would reflect the viscosity data at high volume fraction of the more viscous component, whereas the fluidity model would reflect the viscosity data at high volume fraction of the lower viscous component. The log additivity model should hold for miscible systems. Actually, viscosity data often deviate from the upper additivity and lower fluidity model bounds. Emulsion theories lead to a positive deviation from additivity model, and absence of adhesion between the phases leads to negative deviation from fluidity model [3]. Razavi Aghjeh et al. [7] observed both additive and negative deviation of the complex viscosity and storage modulus (measured at $0.1\ s^{-1}$) of a high-density polyethylene (HDPE)/high-impact polystyrene (HIPS) blend, depending on the amount of HIPS (Fig. 16.1). This type of behavior (that is to say negative followed by positive deviation behavior) is usually observed

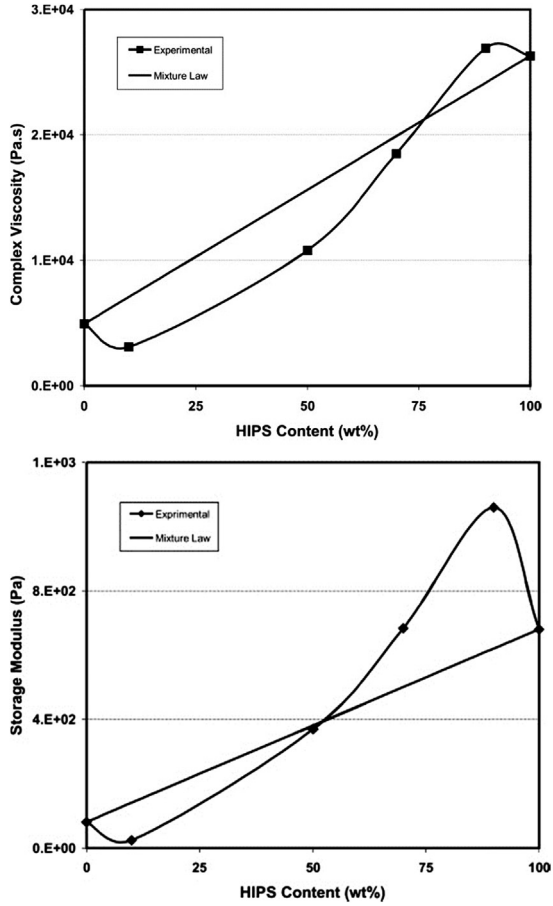

Figure 16.1 Complex viscosity and storage modulus versus high-impact polystyrene content obtained from experimental rheological results and calculated values using additive mixing rule at $\omega = 0.1\ s^{-1}$. *(Reproduced from Aghjeh MKR, Khodabandelou M, Khezrefaridi M. Rheology and morphology of high impact polystyrene/polyethylene blends and the effect of compatibilization on their properties. J Appl Polym Sci 2009;114:2235–2245. https://doi.org/10.1002/app.30629. with permission of John Wiley and Sons.)*

when the interfacial interaction between polymer phases is affected by the blend composition. The negative deviation is related to a poor interfacial interaction between polyethylene (PE) and the different types of dispersed phases, whereas positive deviation of viscosity and elastic modulus for high HIPS content blends was attributed to the interfacial and hydrodynamic interactions between dispersed PE and polybutadiene (PB) particles [8].

Positive deviation can be observed in miscible blends comprising components with similar chemical structures but different chain topology, such as a metallocene-catalyzed linear low-density polyethylene (mLLDPE)/low-density polyethylene (LDPE) blend [9]. In another example, incompatible polystyrene (PS)/PE blends show negative deviation from additive mixing rule in all the blend composition due to the low interfacial interaction between the phases [10].

Hence, the shape of the complex viscosity versus frequency under dynamic rheological tests can give information on the interfacial adhesion between both components of a blend. For example, Hassanpour Asl et al. [11] plotted $\eta^* = f(\omega)$ for HDPE/polyamide 6 (PA 6) and HDPE/poly (ethylene-*co*-vinyl alcohol) (EVOH) blends with various amounts of each polymeric phase from 0/100 to 100/0. The authors noted that the viscosity plots corresponding to noncompatibilized HDPE/PA 6 blends were located between those of parent polymers, suggesting a poor interfacial adhesion. Moreover, the viscoelastic behavior was governed by the more viscous phase (HDPE rather than PA 6). On the contrary, due to the similarity between ethylenic parts of the EVOH random copolymer and HDPE chains, the state of entanglement together with the nonpolar interactions between ethylenic segments of the two polymers determined the viscoelastic behavior of the blend (Fig. 16.2).

The shape of the G′ and G″ curves versus pulsation (ω) for pure polymers, with monodispersed linear architecture, in the terminal zone,

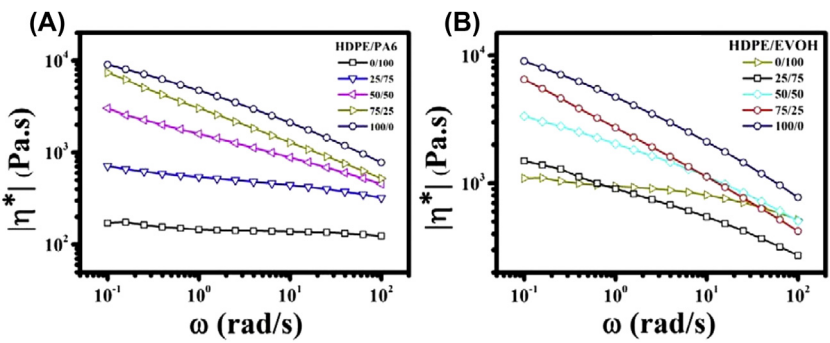

Figure 16.2 Complex viscosity of neat constituents and noncompatibilized binary blends. (A) high-density polyethylene (HDPE)/polyamide 6; (B) HDPE/poly(ethylene-*co*-vinyl alcohol). *(Reproduced from Hassanpour Asl F, Saeb MR, Jafari SH, Khonakdar HA, Rastin H, Pötschke P, et al. Looking back to interfacial tension prediction in the compatibilized polymer blends: discrepancies between theories and experiments. J Appl Polym Sci 2018;46144:1—10. https://doi.org/10.1002/app.46144. with permission of John Wiley and Sons.)*

leads to $G' \propto \omega^2$ and $G'' \propto \omega$ (in a double-logarithmic plot) [12], whereas it is not the case for branched polymers and for polymer blends [13].

Usually, in the case of matrix/dispersed phase, at high frequency, both storage and loss moduli of the blend are quite close to that of the matrix. However, at low frequency, additional relaxation processes are often characterized by a shoulder in the storage modulus [12]. In other words, it is often observed that the deformation of the droplets of the minor phase leads to an increase of the storage modulus at low frequency for the blend [13,14]. The process associated with the reformation of a deformed particle to its primarily spherical form is called the form relaxation process. The shape relaxation behavior of the dispersed droplets was evidenced for many different blends (polydimethyl siloxane (PDMS)/ethylene–octene copolymer (POE), PDMS/polyisobutylene (PIB), PS/PE, polypropylene (PP)/PS, poly(lactic acid) (PLA)/poly(butylene adipate-*co*-terephthalate) (PBAT), PLA//poly(butylene succinate-*co*-adipate) (PBSA), PS/polyamide (PA), PS/poly(methyl methacrylate) (PMMA), PA/poly(styrene-*co*-acrylonitrile) (PSAN), PLA/polyethylene terephthalate glycol (PETG), polycarbonate (PC)/styrene–acrylonitrile (SAN), PC/PS…) [15]. The form relaxation process possesses a characteristic time τ_1, the form relaxation time, which is larger than the terminal relaxation times of the blend components. For example, the interfacial relaxation time for both PLA/PBAT and PLA/PBSA was around 8s, whereas the relaxation time of PLA was around 0.05s (Fig. 16.3) [13].

The relaxation time λ_D for the drop shape is given by the following Eq. (16.1).

$$\lambda_D \sim f(p)\frac{R\,\eta_m}{\Gamma} \tag{16.1}$$

Then, relaxation time (λ_D) depends on the particle radius, R, the viscosity of the matrix, η_m, the viscosity of the minor phase, η_d, and the interfacial tension. Palierne model is an emulsion model based on the linear viscoelastic properties of blends and takes into account the influence of the interfacial tension on the complex modulus [16]. To use Palierne model, the viscosity ratio must be close to 1. Because if the dispersed phase is too viscous (thermoplastic elastomers [TPE] for example), the droplets do not deform and the model cannot be used. Eq. (16.2) expresses $G^*(\omega)$ as a function of ω (the frequency in rad.s^{-1}) using $H_i(\omega)$ given in Eq. (16.3):

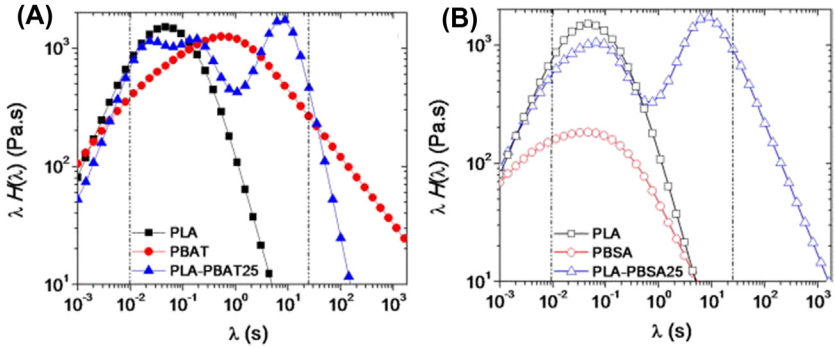

Figure 16.3 Time-weighed relaxation spectra λH(λ) versus λ of (A) poly(lactic acid) (PLA), poly(butylene adipate-*co*-terephthalate) (PBAT) and 75/25 PLA/PBAT blend, and (B) PLA, poly(butylene succinate-*co*-adipate) (PBSA) and 75/25 PLA/PBSA blend. *(Reproduced from Nofar M, Maani A, Sojoudi H, Heuzey MC, Carreau PJ. Interfacial and rheological properties of PLA/PBAT and PLA/PBSA blends and their morphological stability under shear flow. J Rheol 2015;59:317–333. https://doi.org/10.1122/1.4905714. with permission of AIP Publishing.)*

$$G^*(\omega) = G_m^*(\omega)\frac{1+3\sum_i \Phi_i H_i(\omega)}{1-2\sum_i \Phi_i H_i(\omega)} \tag{16.2}$$

$$H_i(\omega) = \frac{4\,\Gamma\, r_i^{-1}\left[5\,G_d^*(\omega)+2\,G_m^*(\omega)\right]+\left[G_d^*(\omega)-G_m^*(\omega)\right]\left[19\,G_d^*(\omega)+16\,G_m^*(\omega)\right]}{40\,\Gamma\, r_i^{-1}\left[G_d^*(\omega)+G_m^*(\omega)\right]+\left[2G_d^*(\omega)+3G_m^*(\omega)\right]\left[19\,G_d^*(\omega)+16\,G_m^*(\omega)\right]} \tag{16.3}$$

where, $G_d^*(\omega)$ and $G_m^*(\omega)$ are the complex moduli of the dispersed phase and the matrix, respectively, Γ is the interfacial tension, and Φ_i the volume ratio of the droplets with the radius r_i.

Many articles deal with the use of Palierne model to evaluate the interfacial tension of blends. For example, Bousmina compared five techniques to determine the interfacial tension in a PS/PA 6 blend [17]. The rheological method has the advantage of being more representative than the other methods as it averaged the behavior over the total interface in the blend rather than considering only one drop or thread or fiber. The limitations are that the secondary plateau in G' must be experimentally accessible, depending on the torque and frequency range. The use of Palierne model to obtain the interfacial tension between PS and PE showed that since the sensitivity of the model is significant in the low-frequency

region, measurements are very long to carry out [14]. The polymers must be thermally stable, and morphology changing must be minor.

Even if Palierne [18] is the most popular emulsion model based on linear viscoelastic behavior of polymer blends [11,19,20], there are other emulsion models such as Choi and Schowalter (for semidilute emulsions of Newtonian liquids) [21–23], Oldroyd's [24], Bousmina's [25], but also Lee and Park's model, Gramespacher and Meissner's model (simply named G–M's model) [26,27]. The G–M's model for example considers that the viscoelastic properties of the blend are constituted of the complex shear modulus of the components and that of the interface. None of these models allow predicting dynamic modulus of cocontinuous morphology.

There are many books and articles dealing with the rheology of either polymer blends [28–31], especially thermosetting blend systems [32], theoretical rheological behavior [3,6,30], or rheology of nanocomposites [33,34] with also theoretical aspects [30].

But the literature on the rheology of compatibilized polymer blends is not so abundant [35–38], especially for nanofillers used as compatibilizers [39–41].

16.3 The case of compatibilization by copolymers

There are several parameters influencing the rheological response of a polymeric compatibilized blend, such as the structure, molecular weight and concentration of the copolymer, the nature of the interfacial interactions, the composition, the state of dispersion, and the distribution. Most of the rheological data in the literature are limited to oscillatory shear measurements under small amplitude of deformation in the molten state. Moreover, it is impossible to draw a general conclusion about the effect of the compatibilizer on the rheological behavior of blends even if some high tendencies exist.

The study of form relaxation processes based on the results of rheological tests performed on compatibilized systems is contradictory. Indeed, emulsion theories are based on spherical inclusions, and the addition of a compatibilizer can deform the dispersed phase. Moreover compatibilized blends cannot be described by emulsion models because the addition of a compatibilizer has consequences on the relaxation time and the rheological properties (dynamic modulus).

At that stage it is important to differentiate three different ways of compatibilization for polymer blends: the addition of (1) block copolymers

that do not react with any phase of the blend, (2) reactive copolymers, and (3) fillers. Indeed, the rheological behavior of those three categories of compatibilization is different.

16.3.1 Addition of premade diblock copolymer A—B (physical compatibilization)

Many articles deal with the linear viscoelastic behavior of polymer blends compatibilized by nonreactive polymers. The dynamic viscosity was shown to be very sensitive to the amount and the structure of the nonreactive block copolymer [42]. Some authors reported a decrease in viscosity after addition of block copolymers. It was the case for 80 HIPS/20 HDPE compatibilized with 1%—5% of H77 (a pure diblock copolymer between styrene and butadiene) or H35 (a tapered diblock copolymer consisting in a random copolymer sequence between pure hydrogenated polybutadiene (HPB) and PS blocks) (Fig. 16.4). For HDPE-rich phase (80 HDPE/20 HIPS), this decrease was observed only when compatibilized with 1% of H35 (Fig. 16.4A.). This is particularly evident at low frequency. In the case of 80 HDPE/20 HIPS, the decreases were firstly explained by a complete different morphology when adding H35. Fibrous-type morphology was observed with H35 compared to spheres for unmodified blends. Secondly, both copolymers had different interfacial activity: H35 acts as a solubilizing agent at low concentrations that tended to swell the interface allowing for a

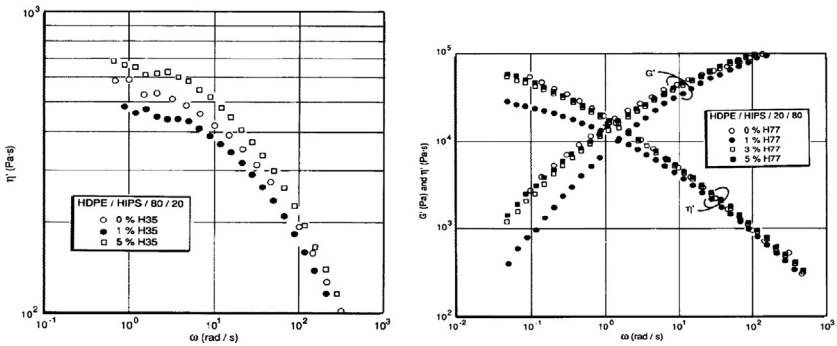

Figure 16.4 Dynamic viscosity η' versus frequency for a 80/20 high-density polyethylene (HDPE)/high-impact polystyrene (HIPS) blend at 180°C with 0%, 1% and 5% of H35 (A) Dynamic viscosity η' and storage modulus G′ versus frequency for a 20/80 HDPE/HIPS blend at 180°C with 0%, 1%, 3% and 5% of H77. *(Reproduced from Brahimi B, Ait-Kadi A, Ajji A, Jérôme R, Fayt R. Rheological properties of copolymer modified polyethylene/polystyrene blends. J Rheol 1991;35:1069—1091. https://doi.org/10.1122/1.550166. with permissions of AIP Publishing.)*

decrease in viscosity, whereas H77 acts as an anchoring agent that allowed for a better adhesion between polymeric phases. At the interfacial saturation concentration, both copolymers had an important contribution to the viscosity increase. At higher amounts than the saturated concentration, the more important increase obtained for the H77 copolymer might be due to its higher molecular weight which induces a higher viscosity and a lower critical micelle concentration (CMC).

On the contrary, some other authors reported an increase in viscosity after addition of a block copolymer to PS/PMMA, PE/PA, PP/PA 6 [43], poly(ethylene terephthalate) (PET)/PA 6 [44], PDMS/PIB [45], or HIPS/HDPE blends. It was explained by an immobilization of the interface, rendering the dispersed phase more rigid particles. More recently, Zhang [46] reported an increase in complex viscosity after addition of 10wt% of a poly(butylene succinate)-*co*-poly(L-lactic acid) (PBS-PLLA) block copolymer into a PLLA/PBS blend, indicating a longer relaxation due to an improved interface interaction between PBS and PLLA. They noted that an excessive addition of a PBS-PLLA copolymer resulted in a reduction of complex viscosity due to the low viscosity of the copolymer. It seemed that the complex viscosity was very sensitive to the molecular weight of the added copolymer. PLA-PBAT-PLA triblock copolymers with high molecular weight led to a better increase in complex viscosity than low molecular weight ones [47]. When the interface between the two polymers is saturated, micelles are formed in the matrix and this can lead to a decrease of the zero-shear viscosity η_0. The formation of micelles in the matrix can also be the result of the process. If one part of the copolymer cannot find its way to the interface (because its migration is too slow due to inappropriate process parameters), the compatibilization is inefficient and the copolymer stays in the matrix forming micelles.

Elastic properties can also be affected by the addition of a compatibilizer [45,48]. Van Hemelrijck studied the influence of various amounts of polyisoprene-block-polydimethylsiloxane (PI-*block*-PDMS) copolymers into PDMS/PI blends on the rheological behavior [37]. He evidenced coalescence with 0.1% of the block copolymer, whereas the 10% compatibilizer led to smaller dispersed phase size. The same authors subjected uncompatibilized and highly compatibilized samples to a preshear at low shear rate until steady state conditions were reached. Subsequently, the shear rate was suddenly increased, and the transient stresses or small-angle light-scattering patterns were recorded as a function of time. An uncompatibilized blend showed a typical increase in N_1 (first normal stress

difference), attributed to the deformation of the droplets into fibril that generated a stronger anisotropy. But as interfacial tension became predominant after a certain period of time, the fibrils started to break up and N_1 decreased until it reached a constant value due to the morphology equilibrium. In the case of a highly compatibilized blend, the stress response was dramatically different. As the droplet did not deform after applying the step-up in shear rate, N_1 kept constant. In the case of an intermediate compatibilizer, the stress response in the molten state was explained based on the occurrence of Marangoni stresses [49]. Regarding the influence of the molecular weight and the length of the blocks of the block copolymer, Van Hemelrijck concluded that coalescence suppression was more effective when the overall molecular weight of the block increased and when the longest block of the block copolymer was located in the matrix [50].

The addition of low amount of nonreactive copolymers into a matrix-dispersed phase blend was shown to lead to an additional relaxation process with a longer relaxation time than the form relaxation one [35]. This relaxation time was related, using an expanded version of the Palierne model, to an interfacial shear modulus. The interfacial relaxation time was shown to increase with molecular weight of the blocks for symmetric block copolymers. Moreover, interfacial relaxation time of an asymmetric block copolymer is longer than for the symmetric one with the same molecular weight [50].

Palierne model was extended to compatibilized polymer blends in order to determine the reduction of interfacial tension brought by a low amount of the copolymer [16].

Bousmina [44] measured the influence of the addition of two types of block copolymers onto the rheological behavior of a blend based on PS and HDPE. Steady shear flow experiments revealed that the addition of the compatibilizer rendered the blend more resistant to flow and then minimized the shear thinning tendency of the blend. This is due to the increase of the interactions because of the interfacial modification. A quantitative comparison between the dynamic viscosity and the steady state shear viscosity shows that the Cox–Merz rule can be applied for the pure components, the blend and the blend modified with 1% of Kraton (styrene–ethylene–butylene–styrene block copolymer (SEBS) triblock copolymer). For those two last cases, it can be applied only for low and intermediate shear rates. The authors evaluated the influence of compatibilizers on transient experiments. As the results of those experiments are greatly affected, they concluded on a large contribution of the relaxation of the modified interface.

Ding et al. [51] plotted the Cole–Cole diagram for an uncompatibilized 70/30 PLA/PBAT blend and the same blend compatibilized with PLA-PBAT-PLA triblock copolymers of low and high molecular weights. Cole–Cole plot often yields two arcs for immiscible blends, which are distributed according to two different relaxation mechanisms corresponding to two different phases. The addition of the triblock compatibilizers to the PLA/PBAT blend results in an incomplete arc in the right side of the diagram assigned to the droplet relaxation. The authors attributed this tail to the droplet–matrix morphology that changes to a cocontinuous morphology in the internal structures.

16.3.2 In situ formation of a block or graft copolymer (reactive compatibilization)

Generally, regarding the evolution of the complex viscosity with reactive compatibilization, there is not only one conclusion. This is due to the great variety of possible reactions and formed reactive species. For example, a viscosity decreasing at high shear rates and increasing at low shear rates after the reactive copolymer addition in PS/PA 6 was revealed [52]. Hassanpour et al. [11] drove almost the same conclusion for an HDPE/PA 6 blend compatibilized with high-density polyethylene–grafted maleic anhydride copolymer (HDPE-*g*-MA). The same authors noted a jump in complex viscosity for modified HDPE (MHDPE)-3.0/EVOH (25% of EVOH and 75% of HDPE modified by 3 phr of MA) and concluded on the optimum effectiveness of the reactive compatibilizer at that rate.

In another article, Zhang et al. [46] noted an increase of the complex viscosity for a PLLA/PBS/PLLA-block-poly(glycidyl methacrylate) (PLLA-*b*-PGMA) compatibilized blend in the entire frequency range compared to an uncompatibilized blend. They concluded that branching and chain extension reaction occurred during processing. The entanglement of the blend with the branched structure was also evidenced by a rubbery plateau. The same conclusion was drawn by Aravind et al. [53] who noted an increase of the complex viscosity of a polytrimethylene terephthalate (PTT)/ethylene propylene diene monomer (EPDM) blend with increasing amounts of maleic anhydride–grafted ethylene propylene monomer (EPM-*g*-MA) in the entire range of frequency. The increase in complex viscosity was taken as an evidence of the interfacial chemical reaction of EPM-*g*-MA. These authors noted a linear increase of G' with compatibilizer addition up to the critical compatibilizer concentration. Beyond this critical concentration, and due to the formation of micelles at higher

concentration, G′ decreases. In the same way, anhydride groups of poly(-styrene-*co*-maleic anhydride) (SMA) are known to react with amino-end groups of PA 6, leading to a dramatic increase of the complex viscosity. Moreover, the viscosity does not reach a plateau at low frequency due to the formation of a network. This is confirmed by the data for the storage moduli G′, which tend to reach a plateau value at low frequencies [54].

As mentioned previously, one of the main fingerprints of the compatibilization in rheology is the low-frequency modulus. Jiang [55] showed that with increasing content of reactive compatibilizer polylactic acid—grafted maleic anhydride (PLA-*g*-MA) in 80/20 PLA/PETG blends, the low-frequency modulus increased gradually. Other authors conducted the same conclusion with PA 6/maleated PP [56]. Jiang et al. explained the increase in interfacial elasticity with compatibilization by a reduction of the dispersed domain size. By this method they isolated the optimum compatibilizing effect (obtained with 3wt% of PLA-*g*-MA) because it led to a maximum of G′ at low frequency.

Moan et al. [38] compared the evolution of the G′ and G″ versus ω without and with various amounts of a random terpolymer (ethylene/acrylic ester/MA) onto an LDPE/polyamide 12 (PA12) blend at a volume fraction $\phi_d = 30\%$. Especially, they observed a plateau at low frequency for G'. By plotting the relaxation spectra H(λ) versus λ, they identified a first shoulder λ_d assigned to the relaxation of PA12 dispersed phase that was slightly shifted toward a higher time in comparison to uncompatibilized blend. They also observed an additional peak λ_{int} at longer time than λ_d. λ_{int} increased with the concentration of added terpolymer up to a certain ϕ_c value and with the molecular weight of the terpolymer at a fixed ϕ_c.

Recently, Nasrollah et al. [57] works on the compatibilization of a PDMS/PI blend using functionalized PDMS and PI copolymers. They used dynamic rheological tests to quantify the chemical reaction between an amine-functionalized polydimethylsiloxane and a MA—functionalized polyisoprene at high temperatures. Especially, they estimated the reaction conversion X of the copolymers into the blend as a function of time using complex viscosity profiles.

Sharma et al. [58] investigated rheological tests under a piston-type capillary rheometer. They plotted the shear stress τ_w versus the true shear rate $\dot{\gamma}_w$ for polybutylene terephthalate (PBT)/SEBS blends compatibilized with styrene—ethylene—butylene—styrene block copolymer—grafted maleic anhydride (SEBS-*g*-MA). A stronger interfacial adhesion and a finer phase morphology resulted in an increased shear stress and melt viscosity.

Other investigations on a capillary rheometer mounted in an industrial injection machine were performed on PET/SBR blends with styrene butadiene rubber (SBR) grafted with MA groups [59]. While the addition of 20–50 phr of SBR to PET had the clear tendency to increase the viscosity regarding pure PET, the reactive compatibilization decreased the viscosity for low and high rubber contents. Indeed, in the first case, the rubber particles induced an increase resistance to flow, whereas in the second case, the reactive compatibilization induced alcoholysis reaction with the terminal hydroxyl groups of PET. This impeded coalescence of the rubber particles leads to an overall decrease in the blend viscosity (Fig. 16.5). The authors studied the influence of the MA concentration (at fixed rubber concentration) on the rheological response (log viscosity vs. log shear rate). The blends with 0.5–1.5 phr of MA (with a fixed grafted SBR rubber concentration of 10 phr) lie above the PET viscosity curve, whereas the blends with 2–3.5 phr of MA exhibit a smaller viscosity than that of PET. Assuming that the MA concentration used in the grafting reaction is proportional to the percentage of MA grafted in the unsaturated butadiene chain, a critical concentration of 2% can be determined. And, a lower viscosity obtained from this 2% concentration may be the result of a

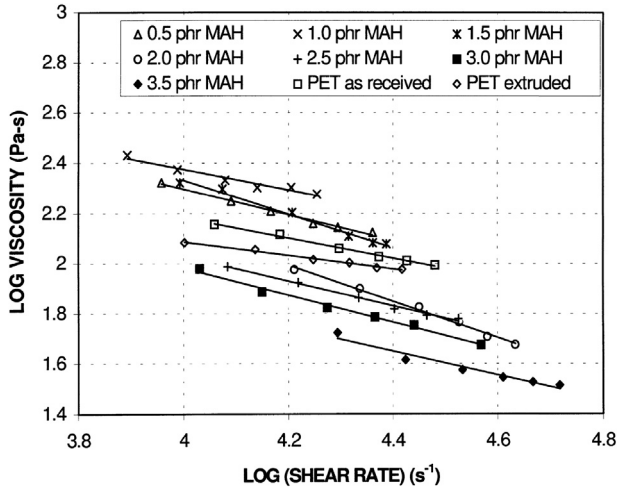

Figure 16.5 Viscosity versus shear rate of poly(ethylene terephthalate)/styrene–butadiene rubber-*g*-maleic anhydride (MA) blends with various phr of MA added as a compatibilizer. *(Reproduced from Sánchez-Solís A, Calderas F, Manero O. Influence of maleic anhydride grafting on the rheological properties of polyethylene terephthalate-styrene butadiene blends. Polymer 2001;42:7335–7342. https://doi.org/10.1016/S0032-3861(01)00197-5. with permissions of Elsevier.)*

better dispersion with inhibited coalescence. The authors also exploited log viscosity versus log shear rate results in order to evaluate the extrusion speed influence of a blend containing 15 phr of SBR with a 2 phr of MA. As expected, higher extrusion speed (50–125 rpm) leads to lower viscosity due to a lower SBR particle diameter. A steep drop in the diameter was observed around 50 rpm, from 20 to 6 μm.

Palierne model was used to evidence the decrease of interfacial tension from 10 mN/m in a nonreactive PP/PA 6 blend to 8 mN/m and then 3 mN/m in a reactive blend with increasing extent of reaction. The compatibilizer was a maleated polypropylene [56]. In other works, the deviation of the Palierne model at low frequency was interpreted by the potential formation of copolymers formed by a reaction between each polymeric phase. This is the case for PLA/PBAT blends that lead to PLA-PBAT copolymer formation stemming from the transesterification between PLA and PBAT [60].

16.3.3 Cocontinuous blends compatibilized with copolymers

Viscoelastic properties can be evaluated in order to discuss the phase morphologies in polymer blends and especially the formation of a cocontinuous morphology. Indeed, G' is very sensitive to the formation of a cocontinuous network [61,62]. Steinmann [61] defended that among the dynamic viscosity (elastic G' and the viscous G'' moduli), G' criterion is the most robust and suitable one to determine the phase inversion concentration for PS/PMMA and poly(styrene-*co*-acrylonitrile (PSAN)/PMMA blends. However, it must be noticed that cocontinuous morphologies are very unstable due to the natural tendency of the melted blends to form a matrix/dispersed phase morphology. Hence, these morphological changes during the measurements render the rheological characterization difficult.

Owing to this difficulty, Velankar et al. studied the viscoelastic behavior of PDMS/PIB blends near the phase inversion and noticed that the addition of a block copolymer as a compatibilizer dramatically increases the complex viscosity far larger compared to "dilute" blends [63]. They attributed this difference to the hydrodynamic interaction between drops. A new model was developed by Yu et al. [64] that allowed to describe the linear viscoelastic behavior of cocontinuous blends. In this model, the interfacial contribution to the dynamic modulus was considered to be quite important at low oscillatory frequency. This model was validated, by comparing

experimental and modeled data for PS/poly(ethylene-*co*-1-octene), PS/PMMA, PS/PSAN, and PLA/poly(ε-caprolactone) (PCL) blends.

16.4 Compatibilization by nanofillers

16.4.1 Rheological properties of polymer-based nanocomposites

There are lots of articles or book chapters dealing with the rheological behavior of NP-filled polymers, especially general reviews [29,34,65–69]. Viscoelastic properties in the molten state are known to be highly influenced by the structure of nanocomposite materials, especially the combination of the mesoscopic structure and the strength of the interaction between the polymer and the NPs [33].

The most singular rheological behaviors of NPs-filled polymers (NPFP) [33] are (1) the changing in the relaxation spectra obtained from the loss and elastic modulus, (2) the shift of nonlinear domain to lower strains with the increase of nanofillers (Payne effect) [65], and (3) the dramatic increase of the complex viscosity at low frequency (nonterminal zone of relaxation) [70]. The former is due to the mobility restriction of polymeric chains when adding nanofillers. The latter was well documented in the literature and has been frequently attributed to the formation of a network consisting of highly dispersed NPs. This is usually attributed to the formation of a percolated particle network of the filled particles obtained by the process. Many parameters influence these behaviors, particularly the size and shape of the NPs and their aspect ratio. Indeed, high aspect ratio particles, such as layered silicates, graphene, or carbon nanotubes, have a propensity to alignment under shear that would decrease the moduli under application of large amplitude oscillatory shear [71].

16.4.2 The localization of nanofillers into a blend

NPs are now classically used to compatibilize polymer blends. The compatibilizing effect of nanofillers is identified by a reduction of the size of the dispersed phase combined with a reduction of the interfacial tension [72] and an improvement of the interfacial adhesion between the two polymeric phases. The efficiency of a nanofiller as a compatibilizer depends on their shape, specific surface area, surface chemistry, and on their localization in the blend. Moreover, one have to keep in mind that the localization depends not only on the shape, aspect ratio, and surface chemistry of the NPs but also on the processing parameters. As mentioned earlier, NPs used as

compatibilizers usually refine the dispersed phase size, thanks to the emulsification role. This is mainly due to coalescence inhibition. The compatibilizing effect of nanofillers is possible if they are localized at the interface. This efficiency as compatibilizers can be quantified by performing rheological tests on the filled blend.

The final localization of a NP into a blend can be predicted by calculating the wetting parameter [41]. This wetting parameter is based only on thermodynamic parameters: the surface tension and hence interfacial tension of the three components. However, as mentioned earlier, the shape and aspect ratio of the NP and the processing parameters play a crucial role in the final dispersion of the NPFP. It was proven by Elias et al. [73] that shear-induced collision of the particles and the dispersed polymer droplets and particle trapping during the coalescence of two droplets are predominant factors compared to diffusion that guided the migration mechanisms of a silica NP from PP to poly(ethylene-*co*-vinyl acetate) (EVA) in a PP/EVA blend. These conclusions were highlighted by Göldel et al. [74] for a low interfacial and cocontinuous blend based on PC, SAN, and multiwall carbon nanotubes (MWCNT). The same authors also showed the influence of the curvature of the blend on the transfer of carbon black (CB) or MWCNTs through the blend interface. They concluded that low aspect ratio NPs (especially CB in a PC/SAN cocontinuous blend) have a high tendency to segregate at the interface, whereas high aspect ratio NPs (especially MWCNT in a PC/SAN cocontinuous blend) are rapidly transferred from SAN to PC [75].

In different articles, Favis et al. [76–78] studied the influence of several parameters on the final localization of NPs into a matrix/dispersed phase polymer blend. The parameters were the interfacial tension between polymers, the size and shape of the NPs, and the mixing sequences.

Once the localization of the NPs into the blend is established, it must be noticed that it dramatically modifies their rheological behavior. Viscoelastic properties in the molten state can provide information regarding the state of dispersion and localization of the nanofillers [79]. Furthermore, they can also provide an insight of the efficiency of the processing characteristics on the dispersion and then on the final properties.

16.4.3 Rheological properties of silica-filled polymer blends

Generally speaking, in the case of sea–island morphologies, when the nanofillers are dispersed in the droplet dispersed phase, the viscosity and

dynamic modulus of the droplet phase are intended to increase. When the nanofillers are dispersed in the continuous phase, a particle network is intended to dramatically modify the viscosity and dynamic modulus. When particles are localized at the interface, they hinder the coalescence. The influence of the localization of silica NPs in an 80 PS/20 PA 6 blend on the coalescence is illustrated in Fig. 16.6 [80]. Dispersed PA 6 size distribution was measured by a laser diffraction particle size analyzer before and after annealing. Those PA 6 nodules were extracted from three different samples: 80 PS/20 PA6, 80PS/20PA6/3bare silica (hydrophilic silica), and 80PS/20PA6/3-grafted-silica (3-methacryloxypropyltrimethoxysilane—modified silica). Bare silica is localized in the PA 6 phase, whereas, grafted silica is localized at the interface between PS and PA 6. Then, it is shown that in the case of grafted silica, the size of the small PA 6 nodules (<10 μm) is unchanged after annealing, due to the formation of a silica—NPs barrier that impede coalescence of PA 6 droplets.

A given silica particle can prevent coalescence of polymer A in polymer B but not of polymer B in polymer A [81].

The slow down or full suppression of coalescence when NPs are localized at the polymer—polymer interface can be revealed by rheological measurements. Most of the model studies were conducted on nearly Newtonian liquids at room temperature with a long thermal stability. This is the case of model materials PDMS/PIB and polyethylene oxide (PEO)/PIB. Tests performed on PEO/PIB under steady state conditions reveals that at the lower stress level of 50 Pa, the viscosity of the blends increases sharply over that of the particle-free blend (Fig. 16.7). Secondly, the particle-containing blends are severely shear-thinning: raising the stress from 50 to 250 Pa reduces the viscosity of the E35—3.5 (75/35 PIB/PEO with 3.5wt% of silica particles) by almost twofold. The lower viscosity of E35—0.07 and E35—0.17 (0.07 and 0.17wt% of silica particles) blends at low stress is due to a coalescence promotion for those two formulations.

In some cases, silica particles localized at the interface can act as a bridge. In that case, a single particle connects simultaneously two dispersed drops at once [81]. This was shown for a PIB/PDMS blend filled with silica NPs [81,83], PEO/PIB/silica microparticles [82,84], and PB/PDMS [85]. The amount of silica was much under the percolation threshold. For this last case, rheological changes specifically attributed to bridging were isolated. It was shown that an annealing of the neat PIB/PEO blend causes a little change in G' at low frequency, whereas for the OTS-modified particles—filled blend, a plateau of G' was formed at low frequency after annealing

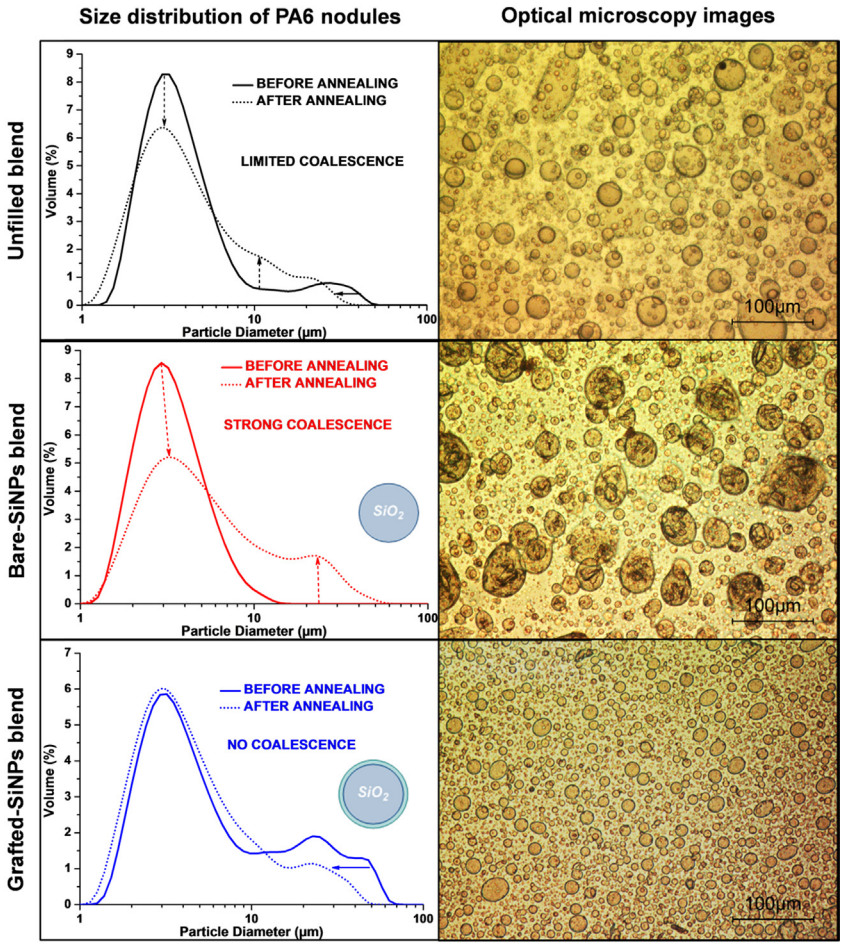

Figure 16.6 Size distribution curves of dispersed polyamide 6 phases before (full lines) and after (dotted lines) annealing using a laser diffraction particle size analyzer for unfilled, bare, and grafted silica nanoparticles (SiNPs) blends (from up to down, respectively). Corresponding morphology (after annealing) obtained by optical microscope for each blend is given in the right column. *(Reproduced form Parpaite T, Otazaghine B, Taguet A, Sonnier R, Caro AS, Lopez-Cuesta JM. Incorporation of modified Stöber silica nanoparticles in polystyrene/polyamide-6 blends: coalescence inhibition and modification of the thermal degradation via controlled dispersion at the interface. Polymer 2014;55:2704–2715. https://doi.org/10.1016/j.polymer.2014.04.016. with permissions of Elsevier.)*

that is characteristic of a yieldlike behavior. And it was explained by the fact that the OTS-modified particles bridge dropped into clusters. Particles aspect ratio (or anisotropy) plays an important role on the coalescence

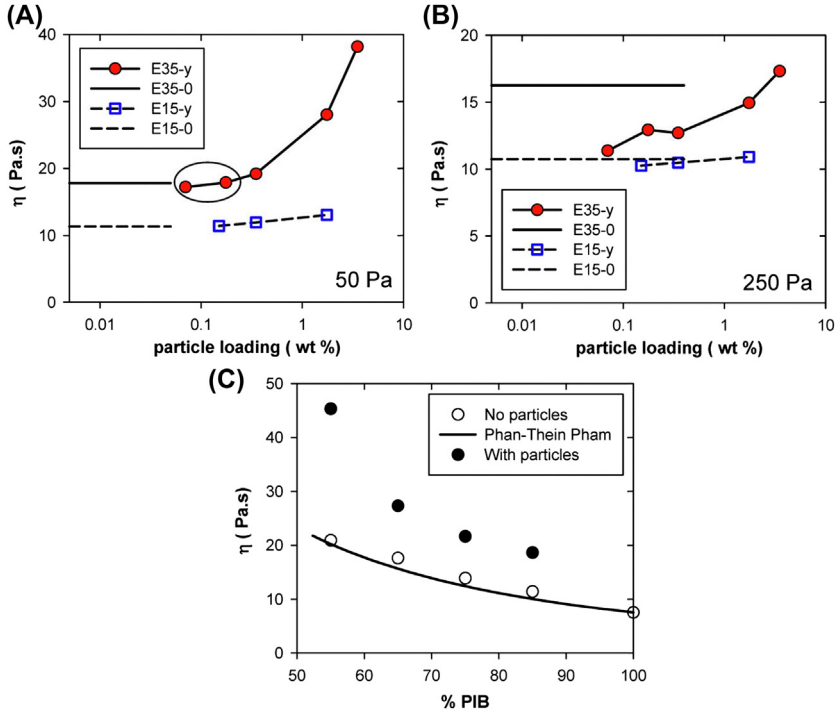

Figure 16.7 Viscosity of polyethylene oxide (PEO)/polyisobutylene (PIB) blends versus silica particles (modified with octadecyltrichlorosilane, OTS) loading for 75/35 PIB/PEO (E35) and 85/15 PIB/PEO (E15) (at 50 Pa stress: A and 250Pa stress: B). And dependence of viscosity on the PIB weight fraction, with or without silica particles modified with OTS (C) Modification of the particles with octadecyltrichlorosilane (OTS) made them preferentially wetted by the PIB phase. *(Reproduced from Nagarkar S, Velankar SS. Rheology and morphology of model immiscible polymer blends with monodisperse spherical particles at the interface. J Rheol 2013;57:901–926. https://doi.org/10.1122/1.4801757. with permissions of AIL Publishing.)*

phenomenon. Anisotropic NPs tend to stabilize blends more efficiently than their spherical counterparts [86].

16.4.4 The case of plate- and tube-shape nanoparticles

The shape and aspect ratio of the NPs play a key role on the refinement efficiency of the dispersed phase [87]. Moreover, it was found that platelike NPs affect the blend morphology much more than spherical ones, especially in the phenomenon of NP-induced cocontinuity. Hence, it is expected that platelets (especially organically modified clays and graphene) and nanotubes (carbon nanotubes) can dramatically affect the rheological

behavior of ternary nanocomposites. As for silica, melt rheology can be used to determine the state of dispersion and localization of organoclays into polymer blends. There are several studies on ternary systems comprising organoclays that examined a strong nonterminal storage modulus. The increase in organoclay content lead to the decrease of the slope of G' versus frequency [88]. As an example, Khoshkava et al. showed a more pronounced nonterminal storage modulus at low frequency with polar Cloisite 30B into PA/PE blends than with Cloisite 15A. They concluded that Cloisite 30B was exclusively localized in the PA matrix and formed a percolated network contrarily to Cloisite 15A [89].

Dynamic rheological measurements combined with microstructure investigation (by scanning electron microscope (SEM) or transmission electron microscope TEM) allow to evidence peculiar morphological transitions induced by NPs [90]. Indeed, the yield stress behavior of filled polymer blends slows down the relaxation leading to thermodynamically unfavorable morphologies. Shape of the NPs is known to play a key role in preserving these peculiar morphologies, even if more investigation would be essential to understand more on the influence of this factor.

Platelet-shape NPs such as organoclay can promote the cocontinuous morphology even at constant amount of polymeric phases. This is ascribed to a change in viscosity ratio and the role of organoclay platelets network formed into the minor phase that prevents the breakup of the minor phase. This was the case for the 70/30 PP/polyamide 6,6 (PA 66) with maleic anhydride–grafted polypropylene (MAPP) blend by adding 10wt% of organoclay [91]. Both percolation of organoclay in PA 66 phase and PA 66 in PP phase (called "double percolation") changed the melt rheological response, especially the plot of storage modulus G' versus loss modulus G''. Curves of G' versus time for a PMMA/PS cocontinuous blend filled with low amounts of Cloisite 15A exhibit a first decrease then an increase up to a steady state value [92]. This shape of the curve is similar to a "bijels" behavior observed for particle jamming at the interface between two partially miscible low-viscosity fluids that undergo spinodal decomposition (as described by Macosko et al. [93]). Hence, at low amounts of Cloisite ($\Phi < \Phi_c$) and during annealing, a first step of coarsening takes place, causing the interfacial crowding of the NPs. Once the interfacial saturation by nanoclays was reached ($\Phi_c = 0.67\%$), rheological measurements (and especially G' vs. frequency) provided information on the elasticity and structure of the percolating network of the system (Fig. 16.8). Above Φ_c, the rheological behavior was dominated by the elastic particle network.

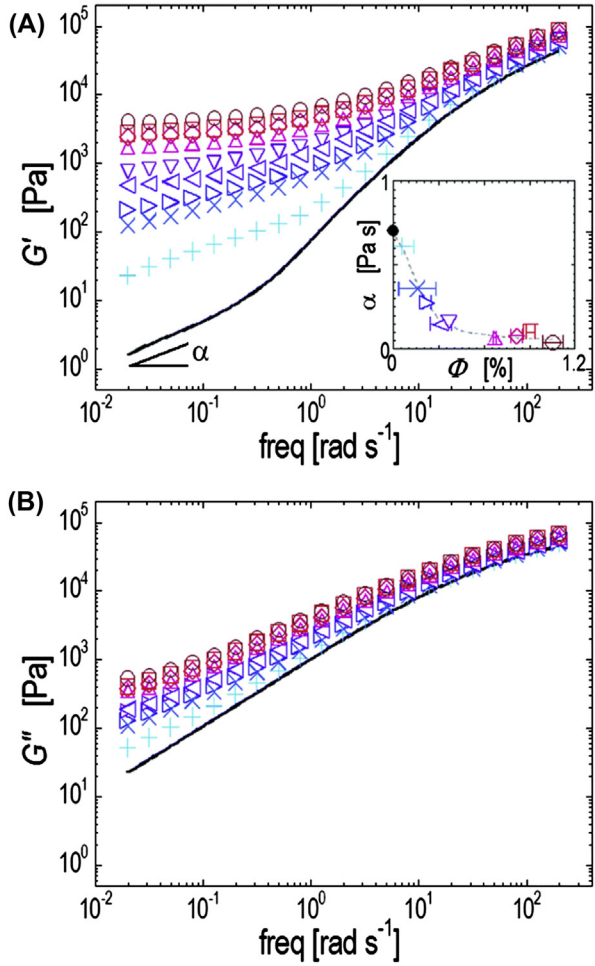

Figure 16.8 Elastic (A) and viscous (B) modulus as a function of frequency for the unfilled blend (solid line) and the filled samples at $\Phi = 0.06$ (plus), 0.16 (cross), 0.22 (right arrow), 0.31 (left arrow), 0.36 (reverse triangle), 0.67 (triangle), 0.81 (diamond), 0.91 (square), and 1.06% (circle). The inset shows the power-law exponents of the low-frequency dependence of the moduli. *(Reproduced from Altobelli R, Salzano de Luna M, Filippone G. Interfacial crowding of nanoplatelets in co-continuous polymer blends: assembly, elasticity and structure of the interfacial nanoparticle network. Soft Matter 2017;13:6465–6473. https://doi.org/10.1039/C7SM01119A. with permissions of Royal Society of Chemistry.)*

Rheological investigation performed on ternary blends comprising nanoclays allows for the identification of an interphase. For example, PE/PA blends with 2 wt% of organically modified montmorillonite exhibit a

time of form relaxation of the PA nodule of 2s, whereas the relaxation time of the interphase was measured (with weighted relaxation spectra) at 15 s and reached 60 s with 4 wt% of organoclays [94].

There are many studies dealing with the addition of carbon nanotubes (CNTs) into immiscible polymer blends. Generally speaking, the conclusions on rheological behavior versus microstructure are the same as similar high aspect ratio NPs. However, rheological and electrical properties of ternary blends comprising CNTs can enquire for the dispersion state and especially the percolation of the threshold of the system [95]. The analysis of weighted relaxation spectra allows for conclusion that the surface of droplets was only partially covered by CNTs. Hence, the uncovered surface relaxes faster than the covered one [96].

16.4.5 Janus Nanoparticles

Different Janus NPs were incorporated into different polymer blends. The Janus NPs can be fully organic [97] or hybrid NPs [98]. They can be spheres or discs [99]. The different examples from the literature are (1) PS/PMMA Janus NPs into PS/PMMA (80/20) blend [97,100], (2) silica Janus NPs into PS/PA 6 (80/20) blend [98,101], (3) PS/PMMA spherical caps into a HDPE/PP (45/45) blend [102], (4) PS/PMMA—modified layered silicate kaolinite into PS/PMMA (30/70) blend [103], (5) triblock terpolymer polystyrene-block-polybutadiene-block-poly(methyl methacrylate) (SBM) Janus NP into poly(2,6-dimethyl-1,4-phenylene ether) (PPE) and poly(styrene-*co*-acrylonitrile) (PSAN) (60/40) [104,105], (6) Janus nanomicelles—based on poly(styrene-*co*-glycidyl methacrylate)-graft-poly(methyl methacrylate) (P((S-*co*-GMA)-*g*-MMA)) into polyvinylidene fluoride (PVDF)/PLLA (50/50) [106,107], (7) Janus hybrid particles (γ-methacryloxypropyltrimethoxysilane-SiO_2@ polydivinylbenzene-dodecyl mercaptan as for MPS-SiO_2@PDVB-DM JPs) into liquid isoprene rubber (LIR)/epoxy resin (ER) (20/80) [108], (8) PS/polyisoprene silica nanosheets into PS/PI (60/40) [109], (9) Janus rubber rybrid particles (PI—SiO_2@PDVB—PB) into PI/PB (60/40) [110], and (10) Janus-polyhedral oligomeric silsesquioxane (POSS) star polymers into PLLA/PCL (70/30) [111].

The singularity of Janus NPs is their capacity to segregate at the interface of an immiscible polymeric blend due to their amphiphilic anisotropic structure comprising two distinct hemispheres [112]. Moreover, Janus NPs have a large desorption energy due to the deep penetration of the grafted

beads into the two different domains of the blend [113]. This control of the location is always followed by a dramatic decrease of the dispersed phase size [97,98], enhancing a high emulsification effect [114]. Moreover, PS/PMMA Janus NPs can stabilize cocontinuous morphology obtained by solvent-evaporation—induced process even after quiescent annealing performed above the glass transition temperature [100]. Indeed, in this study, bicontinuous PS/PMMA morphology was kinetically trapped with tunable domain sizes in drop-cast films beginning as a single phase via solvent-induced demixing. Janus nanosheets have a higher interfacial activity than spherical silica NPs as they reduce the free energy of the system at lower amounts. Only 2 wt% of silica nanosheets are needed to saturate all the interfaces [109].

The low amount (<5 wt%) needed to compatibilize blends sounds like a good opportunity for an industrial use at large scale of this new compatibilizer [104]. Mechanical properties, especially fatigue crack propagation, was dramatically improved by adding both Janus NPs and linear polystyrene-block- polybutadiene-block-poly(methyl methacrylate) (SBM) triblock terpolymers at the interface of a poly(2,6-dimethyl-1,4-phenylene ether)/poly(styrene-*co*-acrylonitrile) (PPE/PSAN) blend [105]. Impact strength was also improved by adding 3 wt% of MPS-SiO_2@PDVB-DM hybrid Janus NPs into LIR/ER thermoset materials [108]. Elongation at break was dramatically improved by adding 3 wt% of poly(styrene-*co*-glycidyl methacrylate)-graft-poly(methyl methacrylate) Janus nanomicelles into (50/50) PLLA/PVDF blend [107]. For example, elongation at break was increased from 3.6 (without any compatibilizer) to 318% (with 3 wt% of Janus nanomicelles) when using simultaneous mixing in the internal mixer.

As discussed previously, Janus NPs are good compatibilizers, and they can also decrease the interfacial tension of the blend. This was proven using dissipative particle dynamics with rigid Janus nanorods of appropriate length [115]. Interfacial tension was measured by some authors using rheological measurement and Palierne model. Parpaite et al. [98] identified a decrease of the interfacial tension between PS and PA 6 from 6.4 to 1.5 mN/m when adding 3 phr of silica Janus NPs. This calculation was performed by assuming that all the Janus NPs segregated at the interface lead to an increase of the volume fraction of PA 6 dispersed phase. The volume fraction was then adjusted using the Kerner model.

In most studies, Janus NPs affect the rheological properties of the blend in the same way as other compatibilizing NPs. That is to say, a gel-like

behavior is identified at low frequency (Fig. 16.9) [98,104]. Bahrami et al. [104] reported a higher increase of complex viscosity for 1, 2, and 5 wt% of Janus NPs into 60/40 SAN/PPE than for 10 wt% (Fig. 16.10). During extrusion, JPs migrate to the PPE/SAN interface. But, at high JP concentration (10 wt%), an excess of JPs forms clusters (supermicelles) in the SAN matrix, facilitating low friction sliding between the PPE droplets and reducing the overall viscosity of the blend. By plotting weighted relaxation spectra it is possible to reveal a "Janus-polymer network" [12] and to identify an interphase relaxation time λ_{int} appearing at much longer time than the shape relaxation of each polymeric phase [101].

More recently, Wang et al. [12] compared the viscous and elastic response of 50/50 PVDF/PLLA blends with different silica NPs (SiO_2 as for unmodified hydrophilic silica NPs, GS as for PLLA-grafted silica NPs and JGS as for Janus-grafted (PLLA/PMMA) silica NPs [116]). PLLA was the matrix whereas PVDF was the dispersed phase; silica NPs were incorporated at an amount of 1 wt%. JGS that were located exclusively at the interface exhibited more elevated moduli and solid-like behaviors contrarily to SiO_2 and GS that were well dispersed in the PLLA matrix. In order to differentiate the contribution of dispersion to that of interparticle interactions, a further analysis based on dynamic modulus study was carried

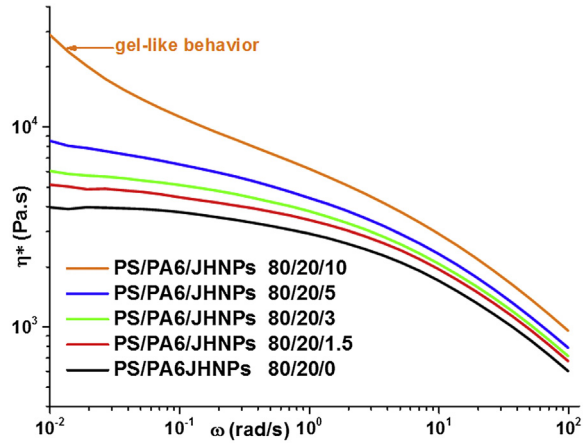

Figure 16.9 Complex viscosity curves of 80 polystyrene (80 PS)/20 polyamide 6 (20 PA 6) blends filled with Janus silica nanoparticles (from 100 to 0.01 rad/s at 230°C). *(Reproduced from Parpaite T, Otazaghine B, Caro AS, Taguet A, Sonnier R, Lopez-Cuesta JM. Janus hybrid silica/polymer nanoparticles as effective compatibilizing agents for polystyrene/polyamide-6 melted blends. Polymer 2016;90:34–44. https://doi.org/10.1016/j.polymer.2016.02.044 with permissions of Elsevier.)*

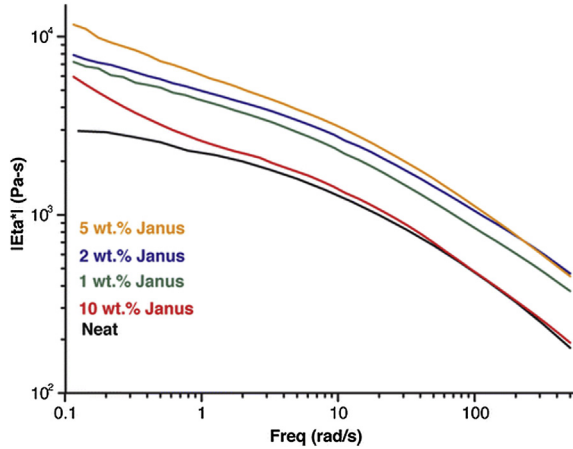

Figure 16.10 Absolute zero shear viscosities of the poly(2,6-dimethyl-1,4-phenylene ether)/styrene–acrylonitrile blends compatibilized with 1, 2, 5, and 10 wt% Janus particles. *(Reprinted with permission from Bahrami R, Löbling TI, Gröschel AH, Schmalz H, Müller AHE, Altstädt V. The impact of Janus nanoparticles on the compatibilization of immiscible polymer blends under technologically relevant conditions. ACS Nano 2014;8:10048–10056. https://doi.org/10.1021/nn502662p. Copyright (2018) American Chemical Society.)*

out. Cole–Cole plot reveals enhanced interaction between JGS and polymer components by molecular entanglements identified by a significant deviation and a long tail in the high $\eta'(\omega)$. Strong flow restriction observed by plotting $\left|\eta^*_{(\omega)}\right| = f\left(\left|G^*_{(\omega)}\right|\right)$ suppresses the deformation of PVDF domains driven by reduced interfacial tension. The same authors also compared the rheological behavior of SiO_2 NPs interfacially confined at the PLLA/PVDF interface with that of PLLA/PVDF/JGS in order to differentiate the effect of the surface chemistry of NPs. Interestingly, the nonterminal behavior was more pronounced for JGS than interfacially jammed SiO_2 NPs. Van Gurp–Plamen, Cole–Cole, and Han plots suggested a more integrated gel-like network with addition of Janus hemispheres onto surface of SiO_2. This was clearly due to the improved interactions among JGS and phase components.

16.5 Conclusions

Rheology and especially oscillatory shear viscosity measurement is a common tool used to characterize the molten state of polymeric systems. It can be used to evidence the compatibilizing effect by using Palierne model

to evaluate the interfacial tension. Moreover, it can indirectly inquire on the behavior of the polymeric system under processing (extrusion, injection). Polymer blends are classically compatibilized by either copolymers (physical or reactive compatibilization) or, more recently, by nanofillers.

The shape, aspect ratio, and surface chemistry of the nanofillers are factors influencing the localization and the interfacial coverage of NPs. Hence, these are all factors that influence the dynamics of assembly, the relaxation phenomenon and the elasticity can be measured by rheological tests. Nanofillers used as compatibilizers enhance a high emulsification effect and stabilize cocontinuous morphology. Platelets shape or nanotubes are known to have a higher interfacial activity than spherical NPs as they reduce the free energy of the system at lower amounts. This can clearly be identified by characterizing the elastic contribution of the viscosity for the system. Rheological measurements can allow differentiating the contribution of the dispersion to that of the interparticle interactions. Hence, it is one of the most efficient tools used to get insight into the interphase in ternary nanocomposites. Among nanofillers, Janus NPs, and especially nanoplatelets or nanotubes, seems to have a huge potential as compatibilizer due to the low amount needed to reach high mechanical properties.

References

[1] Montgomery TS, editor. Introduction to polymer rheology. John Wiley & Sons, Inc.; 2012.

[2] Kontopoulou M, editor. Applied polymer rheology. John Wiley & Sons, Inc.; 2012.

[3] Utracki LA, editor. Polymer blends handbook. Kluwer Academic Publishers; 2002.

[4] Everaert V, Aerts L, Groeninckx G. Phase morphology development in immiscible PP/(PS/PPE) blends influence of the melt-viscosity ratio and blend composition. Polymer 1999;40:6627–44. https://doi.org/10.1016/S0032-3861(99)00048-8.

[5] Han CD. Rheology in polymer processing. Rheol. Polym. Process. New York: Academic; 1976. p. 165–91.

[6] Robeson LM, editor. Polymer belnds. A comprehensive review. Hanser; 2007.

[7] Aghjeh MKR, Khodabandelou M, Khezrefaridi M. Rheology and morphology of high impact polystyrene/polyethylene blends and the effect of compatibilization on their properties. J Appl Polym Sci 2009;114:2235–45. https://doi.org/10.1002/app.30629.

[8] Huang C, Yu W. Rheology and processing of nanoparticle filled polymer blend nanocomposites. In: Thomas S, Muller R, Abraham J, editors. Rheol. process. polym. nanocomposites. Wiley; 2016. p. 491–550.

[9] Fang Y, Carreau PJ, Lafleur PG. Thermal and rheological properties of mLLDPE/LDPE blends. Polym Eng Sci 2005;45:1254–64. https://doi.org/10.1002/pen.20401.

[10] Fayt R, Jérôme R, Teyssié P. Molecular design of multicomponent polymer systems. XIV. Control of the mechanical properties of polyethylene–polystyrene blends by block copolymers. J Polym Sci Part B: Polym Phys 1989;27:775–93. https://doi.org/10.1002/polb.1989.090270405.

[11] Hassanpour Asl F, Saeb MR, Jafari SH, Khonakdar HA, Rastin H, Pötschke P, et al. Looking back to interfacial tension prediction in the compatibilized polymer blends: discrepancies between theories and experiments. J Appl Polym Sci 2018;46144:1–10. https://doi.org/10.1002/app.46144.
[12] Wang H, Yang X, Fu Z, Zhao X, Li Y, Li J. Rheology of nanosilica-compatibilized immiscible polymer blends: formation of a "heterogeneous network" facilitated by interfacially anchored hybrid nanosilica. Macromolecules 2017;50:9494–506. https://doi.org/10.1021/acs.macromol.7b02143.
[13] Nofar M, Maani A, Sojoudi H, Heuzey MC, Carreau PJ. Interfacial and rheological properties of PLA/PBAT and PLA/PBSA blends and their morphological stability under shear flow. J Rheol 2015;59:317–33. https://doi.org/10.1122/1.4905714.
[14] Mekhilef N, Carreau PJ, Favis BD, Martin P, Ouhlal A. Viscoelastic properties and interfacial tension of polystyrene-polyethylene blends. J Polym Sci Part B: Polym Phys 2000;38:1359–68. https://doi.org/10.1002/(SICI)1099-0488(20000515)38:10<1359::AID-POLB130>3.0.CO;2-D.
[15] Omonov TS, Harrats C, Moldenaers P, Groeninckx G. Phase continuity detection and phase inversion phenomena in immiscible polypropylene/polystyrene blends with different viscosity ratios. Polymer 2007;48:5917–27. https://doi.org/10.1016/j.polymer.2007.08.012.
[16] Graebling D, Muller R, Palierne JF. Linear viscoelastic behavior of some incompatible polymer blends in the melt. Interpretation of data with a model of emulsion of viscoelastic liquids. Macromolecules 1993;26:320–9. https://doi.org/10.1021/ma00054a011.
[17] Xing P, Bousmina M, Rodrigue D, Kamal MR. Critical experimental comparison between five techniques for the determination of interfacial tension in polymer blends: model system of polystyrene/polyamide-6. Macromolecules 2000;33:8020–34. https://doi.org/10.1021/ma000537x.
[18] Palierne JF. Linear rheology of viscoelastic emulsions with interfacial tension. Rheol Acta 1990;29:204–14. https://doi.org/10.1007/BF01331356.
[19] Yee M, Calvao PS, Demarquette NR. Rheological behavior of poly(methyl methacrylate)/polystyrene (PMMA/PS) blends with the addition of PMMA-ran-PS. Rheol Acta 2007;46:653–64. https://doi.org/10.1007/s00397-006-0154-7.
[20] Jafari SH, Hesabi MN, Khonakdar HA, Asl-Rahimi M. Correlation of rheology and morphology and estimation of interfacial tension of immiscible COC/EVA blends. J Polym Res 2011;18:821–31. https://doi.org/10.1007/s10965-010-9479-0.
[21] Choi SJ, Schowalter WR. Rheological properties of nondilute suspensions of deformable particles. Phys Fluids 1975;18:420. https://doi.org/10.1063/1.861167.
[22] Graebling D, Froelich D, Muller R. Viscoelastic properties of polydimethylsiloxane-polyoxyethylene blends in the melt. Emulsion model. J Rheol 1989;33:1283–91. https://doi.org/10.1122/1.550051.
[23] Scholz P, Froelich D, Muller R. Viscoelastic properties and morphology of two-phase polypropylene/polyamide 6 blends in the melt. Interpretation of results with an emulsion model. J Rheol 1989;33:481–99. https://doi.org/10.1122/1.550024.
[24] Graebling D, Muller R. Rheological behavior of polydimethylsiloxane/polyoxyethylene blends in the melt. Emulsion model of two viscoelastic liquids. J Rheol 1990;34:193–205. https://doi.org/10.1122/1.550123.
[25] Bousmina M. Rheology of polymer blends: linear model for viscoelastic emulsions. Rheol Acta 1999;38:73–83. https://doi.org/10.1007/s003970050157.
[26] Gramespacher H, Meissner J. Interfacial tension between polymer melts measured by shear oscillations of their blends. J Rheol 1992;36:1127–41. https://doi.org/10.1122/1.550304.
[27] Liao HY, Tao GL, Liu CL, Gong FH. A polypropylene/high density polyethylene blend compatibilized with an ethylene-propylene-diene monomer block copolymer:

fitting dynamic rheological data by emulsion models with a physical scheme. J Appl Polym Sci 2016;133:1–8. https://doi.org/10.1002/app.43709.
[28] Dressler M, Edwards BJ. Rheology of polymer blends with matrix-phase viscoelasticity and a narrow droplet size distribution. J Non-Newtonian Fluid Mech 2004;120:189–205. https://doi.org/10.1016/j.jnnfm.2004.02.009.
[29] Münstedt H. Rheological and morphological properties of dispersed polymeric materials. Munich: Hanser. Hanser Publishers; 2016.
[30] Isayev AI, Palsule S, editors. Encyclopedia of polymer blends. Processing, vol. 2. Wiley; 2011.
[31] Lipatov YS, Shumsky VF, Getmanchuk IP, Gorbatenko AN. Rheology of polymer blends. Rheol Acta 1982;21:270–9. https://doi.org/10.1007/BF01515715.
[32] Thomas S, Grohens Y, Jyotishkumar P, editors. Characterization of polymer blends miscibility, morphology and interfaces. Wiley; 2015.
[33] Krishnamoorti R, Chatterjee T. Rheology and processing of polymer nanocomposites. Wiley; 2016.
[34] Shenoy AV, editor. Rheology of filled polymer systems. US: Springer; 1999.
[35] Riemann R-E, Cantow H-J, Friedrich C. Interpretation of a new interface-governed relaxation process in compatibilized polymer blends. Macromolecules 1997;30:5476–84. https://doi.org/10.1021/ma961814w.
[36] Van Puyvelde P, Velankar S, Moldenaers P. Rheology and morphology of compatibilized polymer blends. Curr Opin Colloid Interface Sci 2001;6:457–63. https://doi.org/10.1016/S1359-0294(01)00113-3.
[37] Van Hemelrijck E, Van Puyvelde P, Moldenaers P. Rheology and morphology of highly compatibilized polymer blends. Macromol Symp 2006;233:51–8. https://doi.org/10.1002/masy.200690028.
[38] Moan M, Huitric J, Médéric P, Jarrin J. Rheological properties and reactive compatibilization of immiscible polymer blends. J Rheol 2000;44:1227–45. https://doi.org/10.1122/1.1289281.
[39] Fenouillot F, Cassagnau P, Majesté J-C. Uneven distribution of nanoparticles in immiscible fluids: morphology development in polymer blends. Polymer 2009;50:1333–50. https://doi.org/10.1016/j.polymer.2008.12.029.
[40] Ginzburg VV. Influence of nanoparticles on miscibility of polymer blends. A simple theory. Macromolecules 2005;38:2362–7. https://doi.org/10.1021/ma0482821.
[41] Taguet a, Cassagnau P, Lopez-Cuesta J-M. Structuration, selective dispersion and compatibilizing effect of (nano)fillers in polymer blends. Prog Polym Sci 2014;39:1526–63. https://doi.org/10.1016/j.progpolymsci.2014.04.002.
[42] Brahimi B, Ait-Kadi A, Ajji A, Jérôme R, Fayt R. Rheological properties of copolymer modified polyethylene/polystyrene blends. J Rheol 1991;35:1069–91. https://doi.org/10.1122/1.550166.
[43] Germain Y, Ernst B, Genelot O, Dhamani L. Rheological and morphological analysis of compatibilized polypropylene/polyamide blends. J Rheol 1994;38:681–97. https://doi.org/10.1122/1.550602.
[44] Iza M, Bousmina M, Jérôme R, Jrôme R. Rheology of compatibilized immiscible viscoelastic polymer blends. Rheol Acta 2001;40:10–22. https://doi.org/10.1007/s003970000112.
[45] Velankar S, Van Puyvelde P, Mewis J, Moldenaers P. Steady-shear rheological properties of model compatibilized blends. J Rheol 2004;48:725–44. https://doi.org/10.1122/1.1765662.
[46] Zhang B, Sun B, Bian X, Li G, Chen X. High melt strength and high toughness PLLA/PBS blends by copolymerization and in situ reactive compatibilization. Ind Eng Chem Res 2017;56:52–62. https://doi.org/10.1021/acs.iecr.6b03151.

[47] Sun Z, Zhang B, Bian X, Feng L, Zhang H, Duan R, et al. Synergistic effect of PLA−PBAT−PLA tri-block copolymers with two molecular weights as compatibilizers on the mechanical and rheological properties of PLA/PBAT blends. RSC Adv 2015;5:73842−9. https://doi.org/10.1039/C5RA11019J.
[48] Wang J, Velankar S. Strain recovery of model immiscible blends: effects of added compatibilizer. Rheol Acta 2006;45:741−53. https://doi.org/10.1007/s00397-005-0038-2.
[49] Lyu S, Jones TD, Bates FS, Macosko CW. Role of block copolymers on suppression of droplet coalescence. Macromolecules 2002;35:7845−55. https://doi.org/10.1021/ma020754t.
[50] Van Hemelrijck E, Van Puyvelde P, Macosko CW, Moldenaers P. The effect of block copolymer architecture on the coalescence and interfacial elasticity in compatibilized polymer blends. J Rheol 2005;49:783−98. https://doi.org/10.1122/1.1888625.
[51] Ding Y, Lu B, Wang P, Wang G, Ji J. PLA-PBAT-PLA tri-block copolymers: effective compatibilizers for promotion of the mechanical and rheological properties of PLA/PBAT blends. Polym Degrad Stabil 2018;147:41−8. https://doi.org/10.1016/j.polymdegradstab.2017.11.012.
[52] Chang F-C, Hwu Y-C. Styrene maleic anhydride and styrene glycidyl methacrylate copolymers as in situ reactive compatibilizers of polystyrene/nylon 6,6 blends. Polym Eng Sci 1991;31:1509−19. https://doi.org/10.1002/pen.760312102.
[53] Aravind I, Jose S, Ahn KH, Thomas S. Rheology and morphology of polytrimethylene terephthalate/ethylene propylene diene monomer blends in the presence and absence of a reactive compatibilizer. Polym Eng Sci 2010;50:1945−55. https://doi.org/10.1002/pen.21723.
[54] Tol R, Groeninckx G, Vinckier I, Moldenaers P, Mewis J. Phase morphology and stability of co-continuous (PPE/PS)/PA6 and PS/PA6 blends: effect of rheology and reactive compatibilization. Polymer 2004;45:2587−601. https://doi.org/10.1016/j.polymer.2003.12.072.
[55] Jiang W, Bao R, Yang W, Liu Z, Xie B, Yang M. Morphology , interfacial and mechanical properties of polylactide/poly (ethylene terephthalate glycol) blends compatibilized by polylactide-g-maleic anhydride. J Mater 2014;59:524−31. https://doi.org/10.1016/j.matdes.2014.03.016.
[56] Asthana H, Jayaraman K. Rheology of reactively compatibilized polymer blends with varying extent of interfacial reaction. Macromolecules 1999;32:3412−9. https://doi.org/10.1021/ma980181d.
[57] Nasrollah Gavgani J, Goharpey F, Velankar S, Foudazi R. Suppressing droplet coalescence and aggregation in immiscible homopolymer blends by interfacially cross-linked compatibilizers. J Rheol 2018;62:1217−31. https://doi.org/10.1122/1.5020961.
[58] Sharma R, Maiti SN. Melt rheological properties of PBT/SEBS and reactively compatibilized PBT/SEBS/SEBS-g-MA polymer blends. J Appl Polym Sci 2015;132:1−11. https://doi.org/10.1002/APP.41402.
[59] Sánchez-Solís A, Calderas F, Manero O. Influence of maleic anhydride grafting on the rheological properties of polyethylene terephthalate-styrene butadiene blends. Polymer 2001;42:7335−42. https://doi.org/10.1016/S0032-3861(01)00197-5.
[60] Al-Itry R, Lamnawar K, Maazouz A. Rheological, morphological, and interfacial properties of compatibilized PLA/PBAT blends. Rheol Acta 2014;53:501−17. https://doi.org/10.1007/s00397-014-0774-2.
[61] Steinmann S, Gronski W, Friedrich C. Quantitative rheological evaluation of phase inversion in two-phase polymer blends with cocontinuous morphology. Rheol Acta 2002;41:77−86. https://doi.org/10.1007/s003970200007.

[62] Pötschke P, Paul DR. Detection of co-continuous structures in SAN/PA6 blends by different methods. Macromol Symp 2003;198:69–82. https://doi.org/10.1002/masy.200350807.
[63] Martin JD, Velankar SS. Effects of compatibilizer on immiscible polymer blends near phase inversion. J Rheol 2007;51:669–92. https://doi.org/10.1122/1.2742391.
[64] Yu W, Zhou W, Zhou C. Linear viscoelasticity of polymer blends with co-continuous morphology. Polymer 2010;51:2091–8. https://doi.org/10.1016/j.polymer.2010.03.005.
[65] Cassagnau P. Melt rheology of organoclay and fumed silica nanocomposites. Polymer 2008;49:2183–96. https://doi.org/10.1016/j.polymer.2007.12.035.
[66] Cassagnau P, Mélis F. Non-linear viscoelastic behaviour and modulus recovery in silica filled polymers. Polymer 2003;44:6607–15. https://doi.org/10.1016/S0032-3861(03)00689-X.
[67] Harrats C, Thomas S, Groeninck G, editors. Micro- and nanostructured multiphase polymer blend systems. Phase morphology and interfaces. CRC Taylor & Francis; 2006.
[68] Song Y, Zheng Q. Linear rheology of nanofilled polymers. J Rheol 2015;59:155–91. https://doi.org/10.1122/1.4903312.
[69] Nazockdast H. Morphology and structure of polymer blends containing nanofillers. In: Isayev AI, editor. Encycl. bolym. blends – vol. 3 struct. WILEY-VCH Verlag GmbH; 2016. p. 401–73.
[70] Ren J, Silva AS, Krishnamoorti R. Linear viscoelasticity of disordered polystyrene–polyisoprene block copolymer based layered-silicate nanocomposites. Macromolecules 2000;33:3739–46. https://doi.org/10.1021/ma992091u.
[71] Ren J, Casanueva BF, Mitchell CA, Krishnamoorti R. Disorientation kinetics of aligned polymer layered silicate nanocomposites. Macromolecules 2003;36:4188–94. https://doi.org/10.1021/ma025703a.
[72] Elias L, Fenouillot F, Majeste JC, Cassagnau P. Morphology and rheology of immiscible polymer blends filled with silica nanoparticles. Polymer 2007;48:6029–40. https://doi.org/10.1016/j.polymer.2007.07.061.
[73] Elias L, Fenouillot F, Majesté J-C, Martin G, Cassagnau P. Migration of nanosilica particles in polymer blends. J Polym Sci, Part B: Polym Phys 2008;46:1976–83. https://doi.org/10.1002/polb.
[74] Göldel A, Kasaliwal GR, Pötschke P, Heinrich G. The kinetics of CNT transfer between immiscible blend phases during melt mixing. Polymer 2012;53:411–21. https://doi.org/10.1016/j.polymer.2011.11.039.
[75] Göldel A, Marmur A, Kasaliwal GR, Pötschke P, Heinrich G. Shape-dependent localization of carbon nanotubes and carbon black in an immiscible polymer blend during melt mixing. Macromolecules 2011;44:6094–102. https://doi.org/10.1021/ma200793a.
[76] Jalali Dil E, Favis BD. Localization of micro- and nano-silica particles in heterophase poly(lactic acid)/poly(butylene adipate-co-terephthalate) blends. Polymer 2015;76:295–306. https://doi.org/10.1016/j.polymer.2015.08.046.
[77] Jalali Dil E, Favis BD. Localization of micro and nano- silica particles in a high interfacial tension poly(lactic acid)/low density polyethylene system. Polymer 2015;77:156–66. https://doi.org/10.1016/j.polymer.2015.08.063.
[78] Jalali Dil E, Arjmand M, Li Y, Sundararaj U, Favis BD. Assembling copper nanowires at the interface and in discrete phases in PLA-based polymer blends. Eur Polym J 2016;85:187–97. https://doi.org/10.1016/j.eurpolymj.2016.09.053.
[79] Bigdeli A, Nazockdast H, Rashidi A, Yazdanshenas ME. Role of nanoclay in determining microfibrillar morphology development in PP/PBT blend nanocomposite fibers. J Polym Res 2012;19:9990. https://doi.org/10.1007/s10965-012-9990-6.

[80] Parpaite T, Otazaghine B, Taguet A, Sonnier R, Caro AS, Lopez-Cuesta JM. Incorporation of modified Stöber silica nanoparticles in polystyrene/polyamide-6 blends: coalescence inhibition and modification of the thermal degradation via controlled dispersion at the interface. Polymer 2014;55:2704–15. https://doi.org/10.1016/j.polymer.2014.04.016.
[81] Vermant J, Cioccolo G, Golapan Nair K, Moldenaers P. Coalescence suppression in model immiscible polymer blends by nano-sized colloidal particles. Rheol Acta 2004;43:529–38. https://doi.org/10.1007/s00397-004-0381-8.
[82] Nagarkar S, Velankar SS. Rheology and morphology of model immiscible polymer blends with monodisperse spherical particles at the interface. J Rheol 2013;57:901–26. https://doi.org/10.1122/1.4801757.
[83] Thareja P, Velankar S. Particle-induced bridging in immiscible polymer blends. Rheol Acta 2006;46:405–12. https://doi.org/10.1007/s00397-006-0130-2.
[84] Thareja P, Velankar S. Rheology of immiscible blends with particle-induced drop clusters. Rheol Acta 2008;47:189–200. https://doi.org/10.1007/s00397-007-0231-6.
[85] Zou Z-M, Sun Z-Y, An L-J. Effect of fumed silica nanoparticles on the morphology and rheology of immiscible polymer blends. Rheol Acta 2014;53:43–53. https://doi.org/10.1007/s00397-013-0740-4.
[86] Vandebril S, Vermant J, Moldenaers P. Efficiently suppressing coalescence in polymer blends using nanoparticles: role of interfacial rheology. Soft Matter 2010;6:3353. https://doi.org/10.1039/b927299b.
[87] Salzano de Luna M, Filippone G. Effects of nanoparticles on the morphology of immiscible polymer blends – challenges and opportunities. Eur Polym J 2016;79:198–218. https://doi.org/10.1016/j.eurpolymj.2016.02.023.
[88] Chow WS, Mohd Ishak ZA, Karger-Kocsis J. Morphological and rheological properties of polyamide 6/poly(propylene)/organoclay nanocomposites. Macromol Mater Eng 2005;290:122–7. https://doi.org/10.1002/mame.200400269.
[89] Khoshkava V, Dini M, Nazockdast H. Study on morphology and microstructure development of PA6/LDPE/organoclay nanocomposites. J Appl Polym Sci 2012;125:E197–203. https://doi.org/10.1002/app.33970.
[90] Pawar SP, Bose S. Peculiar morphological transitions induced by nanoparticles in polymeric blends: retarded relaxation or altered interfacial tension? Phys Chem Chem Phys 2015;17:14470–8. https://doi.org/10.1039/c5cp01644d.
[91] Wang L, Shi C, Guo Z-X, Yu J. Tailoring the morphology of polypropylene/polyamide 66 blend at an asymmetric composition by using organoclay and maleic anhydride grafted polypropylene. J Ind Eng Chem 2014;20:259–67. https://doi.org/10.1016/j.jiec.2013.03.040.
[92] Altobelli R, Salzano de Luna M, Filippone G. Interfacial crowding of nanoplatelets in co-continuous polymer blends: assembly, elasticity and structure of the interfacial nanoparticle network. Soft Matter 2017;13:6465–73. https://doi.org/10.1039/C7SM01119A.
[93] Bai L, Fruehwirth JW, Cheng X, Macosko CW. Dynamics and rheology of nonpolar bijels. Soft Matter 2015;11:5282–93. https://doi.org/10.1039/c5sm00994d.
[94] Ville J, Médéric P, Huitric J, Aubry T. Structural and rheological investigation of interphase in polyethylene/polyamide/nanoclay ternary blends. Polymer 2012;53:1733–40. https://doi.org/10.1016/j.polymer.2012.02.040.
[95] Zonder L, Ophir a, Kenig S, McCarthy S. The effect of carbon nanotubes on the rheology and electrical resistivity of polyamide 12/high density polyethylene blends. Polymer 2011;52:5085–91. https://doi.org/10.1016/j.polymer.2011.08.048.
[96] Tao F, Auhl D, Baudouin A, Stadler FJ, Bailly C. Influence of multiwall carbon nanotubes trapped at the interface of an immiscible polymer blend on interfacial tension. Macromol Chem Phys 2013;214:350–60. https://doi.org/10.1002/macp.201200518.

[97] Walther A, Matussek K, Müller AHE. Engineering nanostructured polymer blends with controlled nanoparticle location using Janus particles. ACS Nano 2008;2:1167–78. https://doi.org/10.1021/nn800108y.
[98] Parpaite T, Otazaghine B, Caro AS, Taguet A, Sonnier R, Lopez-Cuesta JM. Janus hybrid silica/polymer nanoparticles as effective compatibilizing agents for polystyrene/polyamide-6 melted blends. Polymer 2016;90:34–44. https://doi.org/10.1016/j.polymer.2016.02.044.
[99] Walther A, André X, Drechsler M, Abetz V, Müller AHE. Janus discs. J Am Chem Soc 2007;129:6187–98. https://doi.org/10.1021/ja068153v.
[100] Bryson KC, Löbling TI, Müller AHE, Russell TP, Hayward RC. Using Janus nanoparticles to trap polymer blend morphologies during solvent-evaporation-induced demixing. Macromolecules 2015;48:4220–7. https://doi.org/10.1021/acs.macromol.5b00640.
[101] Caro ASS, Parpaite T, Otazaghine B, Taguet A, Lopez-Cuesta JMM. Viscoelastic properties of polystyrene/polyamide-6 blend compatibilized with silica/polystyrene Janus hybrid nanoparticles. J Rheol 2017;61:305–10. https://doi.org/10.1122/1.4975334.
[102] Virgilio N, Favis BD. Self-assembly of Janus composite droplets at the interface in quaternary immiscible polymer blends. Macromolecules 2011;44:5850–6. https://doi.org/10.1021/ma200647t.
[103] Weiss S, Hirsemann D, Biersack B, Ziadeh M, Müller AHE, Breu J. Hybrid Janus particles based on polymer-modified kaolinite. Polymer 2013;54:1388–96. https://doi.org/10.1016/j.polymer.2012.12.041.
[104] Bahrami R, Löbling TI, Gröschel AH, Schmalz H, Müller AHE, Altstädt V. The impact of Janus nanoparticles on the compatibilization of immiscible polymer blends under technologically relevant conditions. ACS Nano 2014;8:10048–56. https://doi.org/10.1021/nn502662p.
[105] Bahrami R, Löbling TI, Schmalz H, Müller AHE, Altstädt V. Synergistic effects of Janus particles and triblock terpolymers on toughness of immiscible polymer blends. Polymer 2017;109:229–37. https://doi.org/10.1016/j.polymer.2016.12.044.
[106] Wang H, Dong W, Li Y. Compatibilization of immiscible polymer blends using in situ formed Janus nanomicelles by reactive blending. ACS Macro Lett 2015;4:1398–403. https://doi.org/10.1021/acsmacrolett.5b00763.
[107] Wang H, Fu Z, Dong W, Li Y, Li J. formation of interfacial Janus nanomicelles by reactive blending and their compatibilization effects on immiscible polymer blends. J Phys Chem B 2016;120:9240–52. https://doi.org/10.1021/acs.jpcb.6b06761.
[108] Xu W, Chen J, Chen S, Chen Q, Lin J, Liu H. Study on the compatibilizing effect of Janus particles on liquid isoprene rubber/epoxy resin composite materials. Ind Eng Chem Res 2017;56:14060–8. https://doi.org/10.1021/acs.iecr.7b03200.
[109] Nie H, Liang X, He A. Enthalpy-enhanced Janus nanosheets for trapping non-equilibrium morphology of immiscible polymer blends. Macromolecules 2018;51:2615–20. https://doi.org/10.1021/acs.macromol.8b00039.
[110] Nie H, Zhang C, Liu Y, He A. Synthesis of Janus rubber hybrid particles and interfacial behavior. Macromolecules 2016;49:2238–44. https://doi.org/10.1021/acs.macromol.6b00159.
[111] Han D, Wen T, Han G, Deng Y, Deng Y, Zhang Q, et al. Synthesis of Janus POSS star polymer and exploring its compatibilization behavior for PLLA/PCL polymer blends. Polymer 2018;136:84–91. https://doi.org/10.1016/j.polymer.2017.12.050.
[112] Yang Q, Loos K. Janus nanoparticles inside polymeric materials: interfacial arrangement toward functional hybrid materials. Polym Chem 2017;8:641–54. https://doi.org/10.1039/C6PY01795A.

[113] Estridge CE, Jayaraman A. Diblock copolymer grafted particles as compatibilizers for immiscible binary homopolymer blends. ACS Macro Lett 2015;4:155–9. https://doi.org/10.1021/mz500793e.
[114] Huang M, Li Z, Guo H. The effect of Janus nanospheres on the phase separation of immiscible polymer blends via dissipative particle dynamics simulations. Soft Matter 2012;8:6834. https://doi.org/10.1039/c2sm25086a.
[115] Zhou C, Luo S, Sun Y, Zhou Y, Qian W. Dissipative particle dynamics studies on the interfacial tension of A/B homopolymer blends and the effect of Janus nanorods. J Appl Polym Sci 2016;133:1–7. https://doi.org/10.1002/app.44098.
[116] Wang H, Fu Z, Zhao X, Li Y, Li J. Reactive nanoparticles compatibilized immiscible polymer blends: synthesis of reactive SiO_2 with long poly(methyl methacrylate) chains and the in situ formation of Janus SiO_2 nanoparticles anchored exclusively at the interface. ACS Appl Mater Interfaces 2017;9:14358–70. https://doi.org/10.1021/acsami.7b01728.